

# Reentrant semiconducting behavior in polymerized fullerites with increasing $sp^3$ content

Jorge Laranjeira,<sup>1,\*</sup> Leonel Marques\*,<sup>1</sup> Manuel Melle-Franco,<sup>2</sup> and Karol Strutyński<sup>2</sup>

<sup>1</sup>*Departamento de Física and CICECO, Universidade de Aveiro, 3810-193 Aveiro, Portugal*

<sup>2</sup>*Departamento de Química and CICECO, Universidade de Aveiro, 3810-193 Aveiro, Portugal*

(Dated: February 28, 2023)

Density functional theory calculations with the hybrid Heyd–Scuseria–Ernzerhof (HSE) functional were used to study the electronic structure of polymerized fullerites, ranging from one-dimensional to three-dimensional polymerized structures. We found that the bandgap across these structures decreases with the rise of the number of  $sp^3$  carbons until metallic behavior is observed. Further increase of the  $sp^3$  carbon content induces a reopening of the bandgap, showing a reentrant semiconducting behavior in this class of materials.

Keywords: DFT Calculations, Carbon Nanostructures, Bandgap Engineering

## INTRODUCTION

The electronic bandgap is responsible for the optical and electronic properties of materials, making it an important parameter to tune in view of possible applications [1, 2]. Bandgap engineering of materials is, therefore, a powerful tool to obtain new physical and chemical properties with possible high technological impact [3, 4].

Carbon materials present distinct electronic properties, from semi-metallic behavior in graphite [5, 6] to the wide bandgap in diamond [7]. Several other carbon allotropes such as peapods, nanotubes and nanoribbons, present a wide range of electronic bandgaps, depending on their structures [8–10]. Solid  $C_{60}$  (fullerite) is a semiconductor and its bandgap decreases under pressure up to 20 GPa, followed by a sudden increase on further compression [11–14]. Saito and coworkers suggested that the initial bandgap decrease is the result of the increasing interaction between  $\pi$  electrons belonging to neighboring molecules induced by the reduction of the molecular distance [11]. Conversely, the sudden rise of the bandgap at 20 GPa is due to the molecular collapse with the formation of an amorphous carbon phase having a high content of  $sp^3$  hybridized atoms [11–13]. Similar behavior has been recently observed in m-xylene solvated  $C_{60}$  [15].

A family of carbon allotropes that have been less studied regarding the electronic structure are the fullerene  $C_{60}$  polymers. Most of these phases have been produced recurring to high-pressure high-temperature (HPHT) treatments of fullerite monomer. Low-dimensional polymers are formed at pressures below 8 GPa. In particular, one-dimensional (1D) orthorhombic polymer and two two-dimensional (2D), tetragonal and rhombohedral, polymers are synthesized with all of them containing 66/66 2+2 cycloaddition bonds, with van der Waals interactions remaining in the non-bonding

directions [16, 17]. Above 8 GPa, three-dimensional (3D) polymerized phases are synthesized [17–23]. Although several 3D phases were reported, very few crystalline structures have been proposed so far. A face-centered cubic (fcc) 3D polymer was synthesized at 9.5 GPa and 550 °C, where the molecules, being in either one of two  $C_{60}$  standard orientations, are bonded through 56/56 2+2 cycloaddition, the cubic structure resulting from the frustrated arrangement of these bonds in the fcc lattice [18, 19]. A cuboidal 3D polymerized phase was synthesized by subjecting the 2D tetragonal polymer to 15 GPa and 600 °C; its proposed orthorhombic structure involves 6/6 3+3 cycloadditions bonds between neighboring molecules belonging to adjacent (a,b) planes and double 66/66 4+4 cycloadditions along the shortest lattice parameter of the (a,b) planes [21]. At the same HPHT conditions, an fcc 3D polymer was synthesized from the fullerite monomer, but it was proposed that it results from the disordering of rhombohedral domains, in which hexagonal planes of molecules are bonded via 5/5 3+3 cycloadditions and 56/65 2+2 cycloadditions are formed between these hexagonal planes [22].

In addition to these fullerite structures, a computationally hypothesized polymerized fullerite clathrate [24] is also to be mentioned since its lattice parameter matches that of an fcc 3D polymer obtained at 12.5 GPa by Brazhkin and coworkers [25]. This clathrate structure is constructed by bonding each molecule, adopting a standard orientation, to the twelve nearest neighbors in the fcc lattice through double 5/5 2+3 cycloaddition bonds.

Here, we report a systematic electronic structure calculations of polymerized fullerite structures ranging from the 1D to 3D polymers, expanding our previous study [26] and performing more accurate electronic structure calculations via the Heyd–Scuseria–Ernzerhof (HSE) hybrid functional [27]. We show that initially, the bandgap progressively decreases with the increasing number of  $sp^3$  carbons until metallic behavior is observed. Then, a further increase in the number of the  $sp^3$  atoms leads to a bandgap reopening in a reentrant behavior, fundamentally similar to the

\* jorgelaranjeira@ua.pt, lmarques@ua.pt

behaviour observed with oxygen functionalized carbon nanotubes [28].

## METHODS

Polymerized fullerite structures were first optimized without any constrain with the Perdew–Burke–Ernzerhof (PBE) [29, 30] exchange-correlation functional augmented with the classical D3 dispersion term [31] with Becke-Johnson damping and a 6-31G(d,p) atomic Gaussian basis set, PBE-6-31G(d,p)-D3, as implemented in CRYSTAL17 [32]. For this, the Coulomb and exchange infinite lattice series is controlled by five numerical thresholds (Ti), which were set to 12 (T1-T4) and 24 (T5). The convergence threshold for the self-consistent field (scf) cycle was set to be smaller than  $10^{-8}$  Hartree and an energy difference of  $10^{-4}$  Hartree was enforced between consecutive geometric steps. A k-point grid with at least  $6 \times 6 \times 6$  points was used for the calculations in bulk systems. In addition, when we computed lower dimensionality systems, namely 1D or 2D self-standing chains, a minimum of 6 points along each periodic direction was used.

As PBE functional systematically underestimates experimental bandgaps [33, 34], the electronic density of states (DOS) and band structures calculations were computed at the HSE06-6-31G(d,p) level [27], which produces improved bandgap values yet with at a feasible computational cost [34]. A denser  $24 \times 24 \times 24$  Monkhorst-Pack [35] grid and a lower scf convergence threshold,  $10^{-10}$  Hartree, were employed for these calculations. Then, band structure calculations were performed with paths from AFLOW [36].

## RESULTS AND DISCUSSION

Table I gives a summary of the optimized structural properties and electronic bandgap values of the polymerized fullerites considered in this study. The optimized polymerized structures are shown in figure S1; their Wyckoff positions are also given in the Supporting Information (SI), section B. The van der Waals fullerite monomer at room conditions is also considered, mainly as a reference, and for simplicity is denoted as 0D [37]. The 3D-AuCu-type and 3D-CuPt-type are ordered structures that have been proposed to be present in the frustrated fcc 3D polymer synthesized at 9.5 GPa and that are described in detail elsewhere [38].

The electronic band structures and densities of states (DOS) for all the polymerized structures being studied are presented in section C of the SI. The low dimensionality polymers bandgap show a strong dependence on the distance between polymeric chains (or layers). We have explicitly investigated the influence of these van der Waals distances on the calculated bandgap for the 1D orthorhombic polymer. Whenever

the distance between the chains is reduced, the bandgap is also reduced and, similarly, when the distance between chains increases the bandgap increases, this being illustrated in figure S11. Moreover, the electronic properties also depend on the orientation adopted by the chains but this was not investigated in this study [17]. To further evaluate the extent to which the van der Waals description influences the bandgaps of low-dimensional polymers, they were computed for the corresponding self-standing polymers, namely: for one molecule, one chain, one quadratic polymerized plane and one hexagonal polymerized plane. The bandgap evolution with the number of  $sp^3$  carbons in the self-standing polymers is shown at the top of figure 1. There is an increase in the bandgaps of the self-standing chains with respect to the bulk system but this difference is reduced when the number of van der Waals interactions decreases. Thus, for the 1D polymerized structure, this has a high impact with its bandgap, 1.85 eV, being now larger than that of the 2D tetragonal polymerized structure, 1.55 eV. This indicates that the smaller bandgap in the bulk 1D polymer is probably an artifact from the chosen theory level description of the van der Waals interaction used here and, indeed, the bandgap decreases monotonously with the number of  $sp^3$  carbons in the low-dimensional polymers. Furthermore, it also allows one to conclude that the observed reduction in the electronic bandgaps of the low-dimensional polymers with the number  $sp^3$  atoms rise is primarily a consequence of the reduction of the intermolecular distance induced by the formation of covalent bonds between the monomers. The reduction in the intermolecular distance leads to a stronger interaction of the molecular wave functions of neighboring molecules leading to an increased dispersion of the bands and the concomitant reduction in the bandgap. In fact, a similar effect has been observed experimentally in compressed monomeric  $C_{60}$  at room temperature [11].

The binary-alloy type structures, 3D-CuPt-type and 3D-AuCu-type, that have been proposed as ordered configurations of the frustrated 3D fcc polymer synthesized at 9.5 GPa, both display metallic behavior at the PBE level [38]. Relevantly, the 3D-CuPt-type polymerized structure has the same number of  $sp^3$  carbons as the 2D-rhombohedral polymerized structure but displays a much smaller bandgap. This is due to the fact that the bonding in this structure being three-dimensional yields a higher band dispersion and a lower molecular volume than that of the 2D-rhombohedral structure, which in turn, induces a stronger interaction of the molecular wave functions, as discussed above.

The 3D-AuCu-type structure, where each molecule is bonded to eight nearest neighbors and has sixteen  $sp^3$  carbons, displays metallic behavior. It is noteworthy to compare this electronic behavior with that of monomeric  $C_{60}$  fullerite compressed at 20 GPa at room temperature, which has about the same volume but is a low-gap semiconductor with a gap of 0.35 eV [14]. This simple comparison indicates that the  $sp^3$  bonding states, absent

TABLE I. Optimized lattice parameters and volume per molecule for the polymerized fullerite structures, at the PBE-6-31G(d,p)-D3 level. The space group of each structure, number of  $sp^3$  carbons per molecule and the electronic bandgap for each structure calculated at the HSE-6-31G(d,p) theory level, are also presented. The hexagonal 3R lattice parameters are used for the rhombohedral structures.

structure	space group	DFT cell constants ( $\text{\AA}$ )	$V(\text{\AA}^3/C_{60})$	# $sp^3$ atoms/ $C_{60}$	Bandgap (eV)
0D	$Fm\bar{3}$	a=14.08 b=14.08 c=14.08 $\alpha = \beta = \gamma = 90$	698.26	0	1.5407
1D	Immm	a=9.11 b=10.29 c=13.99 $\alpha = \beta = \gamma = 90$	655.68	4	1.2580
2D-tetragonal	Immm	a=9.05 b=9.15 c=14.91 $\alpha = \beta = \gamma = 90$	617.96	8	1.3771
2D-rhombohedral	$R\bar{3}m$	a=9.19 b=9.19 c=24.65 $\alpha = \beta = 90; \gamma = 120$	601.45	12	1.1479
3D-CuPt-type	$R\bar{3}c$	a=9.45 b=9.45 c=2x22.34 $\alpha = \beta = 90; \gamma = 120$	576.22	12	0.0628
3D-AuCu-type	$P4_2/mnm$	a=9.27 b=9.27 c=12.87 $\alpha = \beta = \gamma = 90$	553.10	16	–
3D-cuboidal	Immm	a=8.50 b=8.62 c=13.16 $\alpha = \beta = \gamma = 90$	481.92	24	–
3D-rhombohedral	$R\bar{3}$	a=8.92 b=8.92 c=22.35 $\alpha = \beta = 90; \gamma = 120$	513.48	24	1.3796
3D-clathrate	$Pm\bar{3}$	a=12.41 b=12.41 c=12.41 $\alpha = \beta = \gamma = 90$	478.31	48	1.2806

in the compressed  $C_{60}$ , are fundamental for closing the bandgap in polymerized structures driving its metallic behavior. This is further corroborated by the results shown in figure S12 where the bandgap of the monomeric fullerite closes at a lattice length of 11.9  $\text{\AA}$ . However, this gap closure, and the corresponding metallicity, cannot be observed experimentally on compressions at room temperature because the cages collapse into an amorphous phase at 20 GPa for a lattice parameter of about 13  $\text{\AA}$  [12]. In the frustrated 3D fcc polymer each molecule has on average 7.6 bonded near-neighbors, indicating that the molecules adopted more frequently the 3D-AuCu-type configuration (eight bonded nearest-neighbors) than the 3D-CuPt-type configuration (six bonded nearest-neighbors) [19]. Considering this, a metallic behavior would be expected for this 3D fcc phase prepared at 9.5 GPa and 550  $^\circ\text{C}$  and, indeed, it was actually experimentally found by Buga and coworkers

[39, 40].

Another 3D polymerized fullerite showing metallic behavior is the so-called cuboidal structure [21]. However, the 3D-rhombohedral polymerized structure is semiconducting, despite having the same number of  $sp^3$  carbons [22]. The optimized 3D-cuboidal structure has a smaller volume per molecule, which is an important parameter to induce metallic behavior through a strong interaction of wave functions from neighboring molecules. These two 3D polymerized structures have been proposed for the  $C_{60}$  polymers synthesized from the 2D tetragonal polymer compressed at 15 GPa and 600  $^\circ\text{C}$  (the 3D-cuboidal) and from the fullerite monomer subjected to the same conditions (the 3D-rhombohedral) [21, 22]. Yet, the lattice parameters from calculations are significantly different from the experimental ones for both cases, as it was thoroughly discussed for the 3D-cuboidal case [41, 42]. Nevertheless, the metallic nature of the 3D-cuboidal

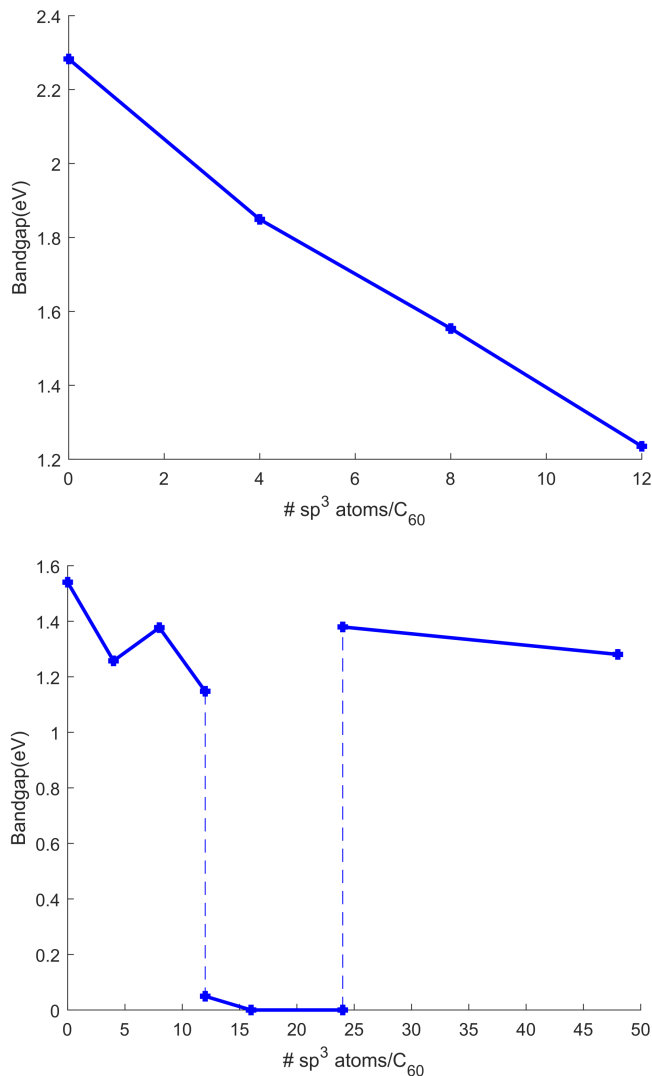


FIG. 1. Top panel: electronic bandgap of the polymerized fullerite structures against the number of  $sp^3$  carbons on each molecule for the self-standing low-dimensional polymers. Bottom panel: same plot for the bulk polymeric systems. The blue line serves only as a guide to the eye.

polymerized phase and the semiconducting behavior of the 3D-rhombohedral polymer were experimentally observed [21, 22].

The last polymerized structure being addressed is the polymerized fullerite clathrate, 3D-clathrate, where most of the atoms are  $sp^3$ - hybridized, forty-eight out of sixty. Thus, likely the  $\sigma$ -like states start to dominate the electronic structure while the few remaining  $\pi$ -like states are highly localized contributing to the semiconducting nature of this structure [24]. It is to be noted that other polymerized structures with higher  $sp^3$  content, having fifty-two, fifty-six and sixty  $sp^3$ -hybridized atoms per molecule, proposed by Burgos and coworkers [43] are also semiconductors, confirming thus the reentrant

semiconducting behavior in polymerized fullerites. These polymerized structures were not investigated by us because they are derived from the body-centered cubic packing, while the experimental structures are based on the fcc packing.

The overall electronic behavior of the polymerized fullerite structures is given in figure 1, bottom panel, where their bandgaps are plotted against their number of  $sp^3$  carbons on each molecule. Initially, the bandgap decreases with the rise of  $sp^3$ -hybridized atoms until its closure, as has been discussed. However, further increase in the number of  $sp^3$  atoms, and concomitantly on the number of polymeric bonds, drives the electronic structure to become dominated by  $\sigma$ -like states, while the remaining  $\pi$ -like states become highly localized, leading to a reopening of the bandgap and a reentrant semiconducting behavior. Although the evolution of the electronic bandgap is dominated by the number of  $sp^3$  carbons on each molecule, the molecular volume alone is also seen to influence the electronic behavior. Polymerized structures with the same number of  $sp^3$  carbons show a considerable reduction in the bandgap, or even its closure, for structures with smaller volumes.

## CONCLUSION

Polymerized fullerite structures present a wide range of electronic behavior from semiconducting to metallic. This behavior is clearly dependent on the number of  $sp^3$  hybridized carbons present in each structure.

The initial reduction of the bandgap with the increment in the number of  $sp^3$  carbons should be a consequence of the  $C_{60}$  intermolecular distance reduction, and concomitantly of the increase in the interaction of the wave functions of neighboring molecules. The bandgap closure is seen to be also determined by the formation of a 3D network of polymeric bonding. Increasing further the number of  $sp^3$  carbons induces a bandgap reopening in a reentrant fashion. This reentrant semiconducting behavior is due to the fact that  $\sigma$ -like states start to dominate the electronic structure, while the remaining  $\pi$ -like states become highly localized.

## ACKNOWLEDGMENTS

This work was developed within the scope of the project CICECO-Aveiro Institute of Materials, UIDB/50011/2020, UIDP/50011/2020 & LA/P/0006/2020, financed by national funds through the FCT/MCTES (PIDDAC) and IF/00894/2015 financed by FCT. J. Laranjeira acknowledges a PhD grant from FCT (SFRH/BD/139327/2018).

- 
- [1] M. Peplow, *Nature* **503**, 327 (2013).
- [2] M. Kang, B. Kim, S. Ryu, S. Jung, J. Kim, L. Moreschini, C. Jozwiak, E. Rotenberg, A. Bostwick, and K. Kim, *Nano Lett.* **17**, 1610 (2017), pMID: 28118710.
- [3] F. Capasso, *Science* **235**, 172 (1987).
- [4] V. Zeghbroeck, *Principles of Semiconductor Devices and Heterojunctions* (Prentice Hall PTR, 2007).
- [5] S. Trickey, F. Müller-Plathe, G. Diercksen, and J. Boettger, *Phys. Rev. B* **45**, 4460 (1992).
- [6] B. Partoens and F. Peeters, *Phys. Rev. B* **74**, 075404 (2006).
- [7] R. Strong, C. Pickard, V. Milman, G. Thimm, and B. Winkler, *Phys. Rev. B* **70**, 045101 (2004).
- [8] M. Otani, S. Okada, and A. Oshiyama, *Phys. Rev. B* **68**, 125424 (2003).
- [9] K. An and Y. Lee, *Nano* **1**, 115 (2006).
- [10] V. Barone, O. Hod, and G. Scuseria, *Nano Lett.* **6**, 2748 (2006).
- [11] Y. Saito, H. Shinohara, M. Kato, H. Nagashima, M. Ohkohchi, and Y. Ando, *Chem. Phys. Lett.* **189**, 236 (1992).
- [12] W. Qiu, S. Chowdhury, R. Hammer, N. Velisavljevic, P. Baker, and Y. Vohra, *High Press. Res.* **26**, 175 (2006).
- [13] F. Moshary, N. Chen, I. Silvera, C. Brown, H. Dorn, M. de Vries, and D. Bethune, *Phys. Rev. Lett.* **69**, 466 (1992).
- [14] M. Núñez–Regueiro, P. Monceau, A. Rassat, P. Bernier, and A. Zahab, *Nature* **354**, 289 (1991).
- [15] Z. Wu, G. Gao, J. Zhang, A. Soldatov, J. Kim, L. Wang, and Y. Tian, *Nano Res.* **15**, 3788 (2022).
- [16] M. Núñez–Regueiro, L. Marques, J.-L. Hodeau, O. Béthoux, and M. Perroux, *Phys. Rev. Lett.* **74**, 278 (1995).
- [17] M. Álvarez–Murga and J.-L. Hodeau, *Carbon* **82**, 381 (2015).
- [18] J. Laranjeira, L. Marques, M. Mezouar, M. Melle-Franco, and K. Strutyński, *Phys. status solidi -RRL* **11**, 1700343 (2017).
- [19] J. Laranjeira, L. Marques, M. Mezouar, M. Melle-Franco, and K. Strutyński, *Mater. Lett.: X* **4**, 100026 (2019).
- [20] L. Marques, M. Mezouar, J.-L. Hodeau, M. Núñez–Regueiro, N. Serebryanaya, V. Ivdenko, V. Blank, and G. Dubitsky, *Science* **283**, 1720 (1999).
- [21] S. Yamanaka, A. Kubo, K. Inumaru, K. Komaguchi, N. Kini, T. Inoue, and T. Irifune, *Phys. Rev. Lett.* **96**, 076602 (2006).
- [22] S. Yamanaka, N. Kini, A. Kubo, S. Jida, and H. Kuramoto, *J. Am. Chem. Soc.* **130**, 4303 (2008).
- [23] V. Blank, S. Buga, G. Dubitsky, N. Serebryanaya, M. Popov, and B. Sundqvist, *Carbon* **36**, 319 (1998).
- [24] J. Laranjeira, L. Marques, M. Melle-Franco, K. Strutyński, and M. Barroso, *Carbon* **194**, 297 (2022).
- [25] V. Brazhkin, A. Lyapin, S. Popova, R. Voloshin, Y. Antonov, S. Lyapin, Y. Kluev, A. Naletov, and N. Mel’nik, *Phys. Rev. B* **56**, 11465 (1997).
- [26] J. Laranjeira and L. Marques, *Mater. Today Commun.* **23**, 100906 (2020).
- [27] V. Barone, O. Hod, J. Peralta, and G. Scuseria, *Acc. Chem. Res.* **44**, 269 (2011).
- [28] S.-H. Jhi, S. Louie, and M. Cohen, *Phys. Rev. Lett.* **95**, 226403 (2005).
- [29] J. Perdew, K. Burke, and M. Ernzerhof, *Phys. Rev. Lett.* **77**, 3865 (1996).
- [30] J. Perdew, K. Burke, and M. Ernzerhof, *Phys. Rev. Lett.* **78**, 1396 (1997).
- [31] S. Grimme, S. Ehrlich, and L. Goerigk, *J. Comput. Chem.* **32**, 1456 (2011).
- [32] R. Dovesi, A. Erba, R. Orlando, C. M. Zicovich-Wilson, B. Civalleri, L. Maschio, M. Rérat, S. Casassa, J. Baima, S. Salustro, and B. Kirtman, *WIREs Comput. Mol. Sci.* **8**, e1360 (2018).
- [33] K. Sohlberg and M. Foster, *RSC Adv.* **10**, 36887 (2020).
- [34] P. Borlido, J. Schmidt, A. Huran, F. Tran, M. Marques, and S. Botti, *Npj Comput. Mater.* **6**, 96 (2020).
- [35] H. Monkhorst and J. Pack, *Phys. Rev. B* **13**, 5188 (1976).
- [36] W. Setyawan and S. Curtarolo, *Comput. Mater. Sci.* **49**, 299 (2010).
- [37] R. Fleming, T. Siegrist, P. Marsh, B. Hessen, A. Kortan, D. Murphy, R. Haddon, R. Tycko, G. Dabbagh, A. Mujsce, M. Kaplan, and S. Zahurak, *MRS Proceedings* **206**, 10.1557/PROC-206-691 (1990).
- [38] J. Laranjeira, L. Marques, N. Fortunato, M. Melle-Franco, K. Strutyński, and M. Barroso, *Carbon* **137**, 511 (2018).
- [39] S. Buga, V. Blank, G. Dubitsky, L. Edman, X.-M. Zhu, E. Nyeanchi, and B. Sundqvist, *J. Phys. Chem. Solids* **61**, 1009 (2000).
- [40] S. Buga, V. Blank, N. Serebryanaya, A. Dzwilewski, T. Makarova, and B. Sundqvist, *Diamond and Related Materials* **14**, 896 (2005), proceedings of Diamond 2004, the 15th European Conference on Diamond, Diamond-Like Materials, Carbon Nanotubes, Nitrides and Silicon Carbide.
- [41] F. Zipoli and M. Bernasconi, *Phys. Rev. B* **77**, 115432 (2008).
- [42] J. Yang, J. Tse, and T. Iitaka, *J. Chem. Phys.* **127**, 134906 (2007).
- [43] E. Burgos, E. Halac, R. Weht, H. Bonadeo, E. Artacho, and P. Ordejón, *Phys. Rev. Lett.* **85**, 2328 (2000).